Available online at www.sciencedirect.com
SCIENCE DIRECT®
Journal of Sound and Vibration 290 (2006) 321–336
JOURNAL OF SOUND AND VIBRATION
www.elsevier.com/locate/jsvi

Accurate analytical type solutions for free vibration frequencies and mode shapes of multi-span bridge decks: the span-by-span approach

D.J. Gorman[a,*], Luigi Garibaldi[b]

[a]*Department of Mechanical Engineering, University of Ottawa, 770 King Edward Avenue, Ottawa, Canada, K1N 6N5*
[b]*Dipartimento di Meccanica, Politecnico di Torino, Corso Duca Degli Abruzzi 24, 10129 Torino, Italy*

Received 3 November 2004; received in revised form 22 March 2005; accepted 31 March 2005
Available online 2 August 2005

Abstract

Utilizing the superposition method an accurate analytical type solution is obtained for the free vibration frequencies and mode shapes of multi-span bridge decks. In this approach to the problem, a separate solution is obtained for the lateral displacement of each individual span. Simple support is provided at the outer extremities of the deck. Conditions of plate continuity and zero lateral displacement are enforced at inter-span support locations. Edges running parallel to the long centre line of the bridge are free. Eigenvalues and mode shapes are presented for a typical bridge deck of three spans, though it is shown that decks of any number of spans may be analysed. Advantages of this approach over an earlier one in which the entire deck was considered as a single plate with intermediate line supports, are discussed. The mathematical procedure developed constitutes one part of an overall study of bridge dynamics. Extension of the analysis to handle orthotropic bridge decks is easily accomplished.

1. Introduction

An ongoing study of the dynamic behaviour of multi-span bridge decks subjected to travelling loads is the subject of research of the second author and his colleagues at the Departimento di

*Corresponding author. Tel.: +1 613 562 5800; fax: +1 613 562 5177.
E-mail address: dgorman@genie.uottawa.ca (D.J. Gorman).

0022-460X/$ - see front matter © 2005 Elsevier Ltd. All rights reserved.
doi:10.1016/j.jsv.2005.03.020

Nomenclature

a_1, a_2	edge lengths of span 1, span 2, etc.
b	width of bridge length
D	plate flexural rigidity $= Eh^3/12(1-\nu^2)$
E	modulus of elasticity of plate material
h	plate thickness
M	bending Moment
Psi	symbol used in figures to represent coordinate ξ
W	plate lateral deflection
ξ	distance along span divided by span length, a_1, a_2, etc.
η	distance across span divided by "b"
λ^2	eigenvalue $= \omega a^2\sqrt{\rho/D}$ where "a" equals span length
λ_b^2	formulation of eigenvalue for storage purposes $= \omega b^2\sqrt{\rho/D}$
ω	circular frequency of vibration
ρ	mass of plate per unit area
ν	Poisson ratio of plate material (taken here as 0.333)
ν^*	$= 2-\nu$
$\phi_1, \phi_2, \ldots$	aspect ratios of first, second, span, etc., $= b/a_1$, b/a_2, etc.

Meccanica of the Politecnico di Torino, of Turin, Italy. Ultimately, the effects on bridge response of surface roughness, etc., and other significant factors will be incorporated into the study.

The main theoretical approach involves computation of bridge deck response by means of modal analysis. An indispensable first step is therefore to develop the ability to establish accurate free vibration frequencies and mode shapes for the multi-span bridge deck. The computation of these frequencies and mode shapes is made more difficult because of the fact that, with a multi-span system, a number of the frequencies may be located very close to each other. Furthermore, in view of the fact that actual bridge deck displacements are measured on functioning bridges, as part of the study, and several of the natural modes may be excited simultaneously, it is of critical importance that each free vibration frequency and mode shape should be accurately identified in advance.

Numerical type solutions for free vibration analysis of multi-span bridge decks had already been available, in particular, solutions based on the finite element method. Nevertheless, the need for a classical analytical type solution, based on continuum mechanics, was well recognized. This latter solution would augment the capabilities of the finite element solution and provide accurate data against which results of the earlier numerical type solution could be compared.

A review of the literature leads one to focus on two possible methods for achieving analytical type solutions. These are the Rayleigh–Ritz method and the superposition method. The superposition method, with which the first author has a number of years of experience, is found to possess a number of attractive features. First, unlike the Rayleigh–Ritz method, it provides solutions which satisfy exactly the governing differential equation throughout the entire domain of the structure. Boundary conditions are satisfied to any desired degree of accuracy by simply increasing the number of terms in the solution. Furthermore, in exploiting the Rayleigh–Ritz method to resolve plate free vibration problems, one typically utilizes the crossed-beam eigenfunctions to represent the plate lateral displacement. Unfortunately, it is known that in the case of plates with opposite free edges, as are encountered here in bridge deck analysis, the free–free beam eigenfunctions do not satisfy exactly the free edge conditions. This is because of the mixed derivatives which appear in the formulation of plate free edge conditions. With the superposition method no such functions are required.

In view of these considerations it has been decided to employ the superposition method in conducting free vibration analysis of bridge decks of interest to the above study. Here a span-by-span approach is taken. The objective of this paper is to describe how the method is exploited to achieve the above goals and the advantages of the span-by-span approach.

It should be clearly understood that the objective set forth here is to develop an analytical procedure for obtaining accurate solutions for the free vibration frequencies and mode shapes of multi-span bridge decks, treated here as a series of thin multi-span plates. It is not the objective of the present paper to undertake the computation of bridge deck response to excitation forces resulting from vehicular traffic or cross winds, etc., a forced vibration problem. The entire paper is devoted to classical free vibration analysis, only.

2. Mathematical procedure

For illustrative purposes we will analyse the three-span thin plate bridge deck as shown in Fig. 1. It will be seen that the analysis is in no way limited in the number of spans which can be handled. The letter "F" in the figure indicates free edges. Other external edges are given simple support while simple transverse line support is provided along the span interfaces. It will be noted that each span has its own coordinate system, span length, and aspect ratio.

In order to analyse the free vibration of this multi-span plate by the superposition method a set of forced vibration solutions (building blocks) are assigned to each span. Later these building blocks will be properly superimposed and a solution to the free vibration problem will be obtained, subject to the condition that all prescribed boundary conditions are satisfied.

The first span of the deck is assigned the building blocks of Fig. 2. The first building block has simple support imposed along its opposite non-driven edges. The other non-driven edge is given

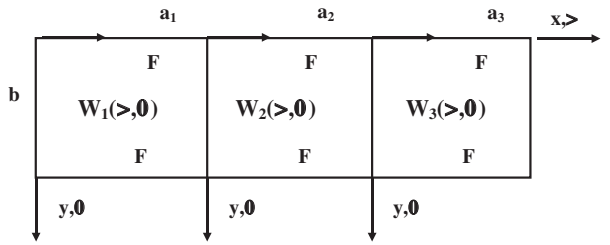

Fig. 1. Typical three-span bridge deck.

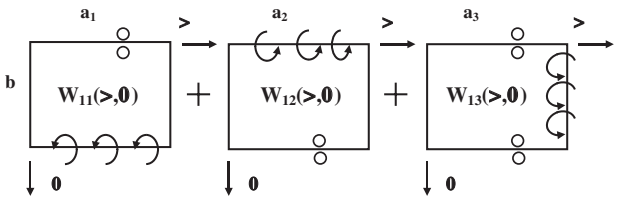

Fig. 2. Building blocks assigned to first span of bridge deck.

slip-shear support, i.e., vertical edge reaction along this edge, as well as slope taken normal to the edge, are everywhere zero. This condition is indicated by two small circles adjacent to the edge. Finally, the driven edge, i.e., the edge, $\eta = 1$, is free of vertical edge reaction but is driven by a distributed harmonic edge rotation of circular frequency ω.

2.1. Development of building block solutions

The solution for spacial distribution of the response of this first building block is taken in the form proposed by Lévy as (see Nomenclature)

$$W(\xi,\eta) = \sum_{m=1,2}^{\infty} Y_m(\eta)\sin(m\pi\xi). \tag{1}$$

The spacial distribution of the enforced harmonic edge rotation is expressed as

$$\left.\frac{\partial W(\xi,\eta)}{\partial\eta}\right|_{\eta=1} = \sum_{m=1,2}^{\infty} E_m \sin(m\pi\xi). \tag{2}$$

Substituting Eq. (1) into the well known thin plate governing differential equation [1], one obtains, for each value of "m", for $\lambda^2 > (m\pi)^2$,

$$Y_m(\eta) = A_m \sinh \beta_m\eta + B_m \cosh \beta_m\eta + C_m \sin \gamma_m\eta + D_m \cos \gamma_m\eta \tag{3}$$

and, for $\lambda^2 < (m\pi)^2$

$$Y_m(\eta) = A_m \sinh \beta_m\eta + B_m \cosh \beta_m\eta + C_m \sinh \gamma_m\eta + D_m \cosh \gamma_m\eta, \tag{4}$$

where $\beta_m^2 = \phi_1^2[\lambda^2 + (m\pi)^2]$, and $\gamma_m^2 = \phi_1^2[\lambda^2 - (m\pi)^2]$, or $\phi_1^2[(m\pi)^2 - \lambda^2]$, whichever is positive. The constants A_m, B_m, etc., are evaluated by enforcement of the prescribed boundary conditions.

It will be obvious, in view of symmetry of the solution about the ξ-axis, that the antisymmetric terms must be deleted from Eqs. (3) and (4). The remaining two boundary conditions to be enforced along the driven edge are formulated as [1]

$$\frac{\partial^3 W(\xi,\eta)}{\partial\eta^3} + v^* \left.\frac{\partial^3 W(\xi,\eta)}{\partial\eta^3\partial\xi^2}\right|_{\eta=1} = 0 \tag{5}$$

and

$$Y'_m(\eta)|_{\eta=1} = E_m, \tag{6}$$

where primes indicate differentiation with respect to η.

Enforcing the first boundary condition above, which expresses a condition of zero vertical edge reaction, we obtain, for $\lambda^2 > (m\pi)^2$

$$Y_m(\eta) = B_m[\cosh \beta_m\eta + \theta_{1m} \cos \gamma_m\eta], \tag{7}$$

where

$$\theta_{1m} = \frac{-\beta_m[\beta_m^2 - v^*\phi_1^2(m\pi)^2]\sinh \beta_m}{\gamma_m[\gamma_m^2 + v^*\phi_1^2(m\pi)^2] \sin \gamma_m}$$

and for $\lambda^2 < (m\pi)^2$

$$Y_m(\eta) = B_m[\cosh\ \beta_m\eta + \theta_{2m}\ \cosh\ \gamma_m\eta], \tag{8}$$

where

$$\theta_{2m} = \frac{-\beta_m[\beta_m^2 - v^*\phi_1^2(m\pi)^2]\sinh\ \beta_m}{\gamma_m[\gamma_m^2 + v^*\phi_1^2(m\pi)^2]\sinh\ \gamma_m}.$$

Imposing the boundary condition represented by Eq. (6) we obtain, for $\lambda^2 > (m\pi)^2$

$$Y_m(\eta) = E_m\theta_{11m}[\cosh\ \beta_m\eta + \theta_{1m}\cos\ \gamma_m\eta], \tag{9}$$

where

$$\theta_{11m} = \frac{1}{\beta_m\ \sinh\ \beta_m - \theta_{1m}\gamma_m\ \sin\ \gamma_m}$$

and for $\lambda^2 < (m\pi)^2$

$$Y_m(\eta) = E_m\theta_{22m}[\cosh\ \beta_m\eta + \theta_{2m}\ \cosh\ \gamma_m\eta], \tag{10}$$

where

$$\theta_{22m} = \frac{1}{\beta_m\ \sinh\ \beta_m + \theta_{2m}\gamma_m\ \sinh\ \gamma_m}.$$

We thus have the exact solution available for response of the first building block to any distribution of imposed harmonic edge rotation at any circular frequency, ω.

Turning to the second building block of Fig. 2 it is seen that it differs from the first only in that the boundary conditions along the edges $\eta = 1$ and $\eta = 0$, are interchanged. It follows then that solution for response of this building block may be extracted from that of the first by simply replacing the quantity, η, of the earlier solution by the quantity, $1 - \eta$, and, because of sign conventions, preceding the new solution with a negative sign.

We now turn to the task of obtaining a solution for response of the third building block of Fig. 2. The opposite non-driven edges of this building block are given slip-shear support. The edge, opposite the driven edge, is given simple support. A condition of zero lateral displacement is enforced along the remaining edge which is driven by a distributed harmonic bending moment.

In order to take advantage of the existing analytical procedure related to the first building block it is found advantageous to obtain a solution for the response of the third building block in the following manner.

We begin by considering building block (a) of Fig. 3. Here also, slip-shear conditions are enforced along the opposite non-driven edges, the remaining non-driven edge is given simple support, and lateral displacement is forbidden along the driven edge which is subjected to a distributed harmonic bending moment.

Amplitude of the distributed bending moment is expressed in dimensionless form as

$$\left.\frac{Mb^2}{a_1D}\right|_{\eta=1} = \sum_{m=0,1,2}^{\infty} E_m\cos\ m\pi\xi, \tag{11}$$

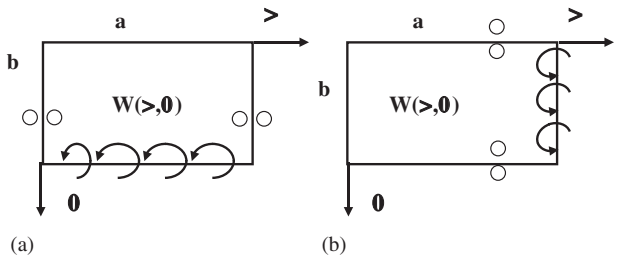

Fig. 3. Building blocks utilized to demonstrate transforming from one building block (a), to another (b).

while solution for the spatial distribution of the building block response is expressed as

$$W(\xi,\eta)=\sum_{m=0,1,2}^{\infty} Y_m(\eta)\cos\, m\pi\xi. \tag{12}$$

It will be obvious to the reader that a solution for the functions $Y_m(\eta)$ of Eq. (12) will take a form identical to that expressed by Eqs. (3) and (4). It will also be obvious that now we must delete these terms in the solution which are symmetric about the ξ-axis. The dimensionless bending moment of Eq. (11) is also expressed as [1,2]

$$\frac{Mb^2}{a_1 D}=-\left\{\frac{\partial^2 W(\xi,\eta)}{\partial\eta^2}+\nu\phi_1^2\,\frac{\partial^2 W(\xi,\eta)}{\partial\xi^2}\right\}. \tag{13}$$

Boundary conditions to be enforced at the driven edge related to lateral displacement and driving moment, respectively, are therefore,

$$Y_m(\eta)|_{\eta=1}=0 \tag{14}$$

and

$$-Y_m''(\eta)|_{\eta=1}=E_m. \tag{15}$$

It is easily shown that the functions $Y_m(\eta)$ are expressed as

For $\lambda^2>(m\pi)^2$

$$Y_m(\eta)=E_m\theta_{11m}[\sinh\,\beta_m\eta+\theta_{1m}\,\sin\,\gamma_m\eta] \tag{16}$$

and $\lambda^2<(m\pi)^2$

$$Y_m(\eta)=E_m\theta_{22m}[\sinh\beta_m\eta+\theta_{2m}\,\sinh\gamma_m\eta], \tag{17}$$

$$\theta_{1m}=-\sinh\beta_m/\sin\gamma_m,$$

$$\theta_{11m}=\frac{-1.0}{\beta_m^2\sinh\,\beta_m-\theta_{1m}\gamma_m^2\,\sin\gamma_m},$$

$$\theta_{2m}=-\sinh\,\beta_m/\sinh\,\gamma_m$$

and

$$\theta_{22m} = \frac{-1.0}{\beta_m^2 \sinh \beta_m - \theta_{2m}\gamma_m^2 \sin \gamma_m},$$

where β_m and γ_m are as defined for the first building block.

It will be apparent that solution for building block (b) of Fig. 3, which is identical to the third building block of Fig. 2, can be obtained through a transformation of the above solution for building block (a). To achieve this end we must transform the solution as follows:

(i) Replace the quantity λ^2 by the product $\lambda^2\phi_1^2$. This is necessary because of the definition of λ^2.
(ii) Replace the aspect ratio ϕ_1 by its inverse.
(iii) Interchange the coordinates η, and ξ.

In view of the coupling of building blocks at the bridge span interfaces, which will be required shortly, it is of utmost importance that we fully understand the nature of the solution which is obtained by the above transformation. The solution for the forced vibration problem of Fig. 3(b) is essentially a mirror image of that of Fig. 3(a). It is important to note that this transformed solution has lateral displacement non-dimensionalized by edge length "b".

The transformed solution takes the form

$$W(\xi,\eta) = \sum_{n=0,1}^{\infty} Y_n(\xi) \cos n\pi\eta, \tag{18}$$

with the driving moment spatial distribution expressed as

$$\frac{Ma_1^2}{bD} = \sum_{n=0,1}^{\infty} E_n \cos n\pi\eta. \tag{19}$$

For $\lambda^2\phi_1^2 > (n\pi)^2$

$$Y_n(\xi) = E_n\theta_{11n}[\sinh \beta_n\xi + \theta_{1n} \sin \gamma_n\xi] \tag{20}$$

and for $\lambda^2\phi_1^2 < (n\pi)^2$

$$Y_n(\xi) = E_n\theta_{22n}[\sinh \beta_n\xi + \theta_{2n} \sinh \gamma_n\xi], \tag{21}$$

$\beta_n^2 = [\lambda^2\phi_1^2 + (n\pi)^2]/\phi_1^2$, and $\gamma_n^2 = [\lambda^2\phi_1^2 - (n\pi)^2]/\phi_1^2$, or $[(n\pi)^2 - \lambda^2\phi_1^2]/\phi_1^2$, whichever is positive.

The quantities θ_{11n}, θ_{1n}, etc. are obtained from the quantifies θ_{11m}, θ_{1m}, etc., related to Eqs. (16) and (17), by merely replacing β_m and γ_m with β_n and γ_n, respectively. Note that we have replaced the subscript "m" with "n" for solutions with analytical functions running in the ξ direction in order to avoid confusion.

We should also observe that for the immediately above solution the dimensionless bending moment acting along the edges, $\eta = 0.0$ and 1.0, will be expressed as [1]

$$\frac{Mb}{D} = -\left\{\frac{\partial^2 W(\xi,\eta)}{\partial\eta^2} + v\phi_1^2 \frac{\partial^2 W(\xi,\eta)}{\partial\xi^2}\right\}, \tag{22}$$

with $\eta = 0.0$ and 1.0, respectively.

We thus have available solutions for the exact response of all building blocks associated with the first span. The above building block solutions are the only ones that will be required in the multi-span plate analysis, regardless of the number of spans involved. Only the aspect ratios may vary as we move from span to span.

Building blocks assigned to internal spans of the multi-span plate will differ from those of Fig. 2 only in that one additional building block will be required. This latter building block will differ from the third one of Fig. 2 only in that it will be moment driven along the edge, $\xi = 0$. Its solution is easily extracted from the third building block above by replacing the quantity ξ, with $1 - \xi$.

Building blocks assigned to the final span of the plate will differ from those assigned to the first span only in that the third building block of Fig. 2 will be replaced by the fourth building block as discussed above for interior spans. The reason for this arrangement of building blocks will become clear shortly.

Before constructing the eigenvalue matrix for the present illustrative three-span problem it will be recalled that our ultimate solution must satisfy free edge conditions along all boundaries running parallels to the ξ-axes. The other conditions to be satisfied are continuity of bending moment and slope as we move across the inter-span lines of support. We employ these conditions to permit generation of the required eigenvalue matrix.

2.2. Development of eigenvalue matrix

The eigenvalue matrix generated for analysis of the three-span deck is shown schematically in Fig. 4. Short horizontal bars indicate non-zero matrix elements. The building blocks utilized and the spans to which they pertain are indicated along the top of the figure. For illustrative purposes it is assumed that three terms are employed in each building block solution.

Elements of the first row of segments in the matrix are based on the required condition of zero net bending moment along the edge, $\eta = 1$, of the first span. Inserts to the right of the figure indicate this condition. Well established procedures for exploiting the superposition method are employed [1]. Each set of building blocks in each span is considered to be superimposed, one-upon-the-other. It will be seen that only the building blocks of the first span can contribute to bending moment along the edge discussed above.

The contribution of each of these building blocks toward this bending moment is expanded in a Fourier sine series of K terms ($K = 3$) of the type utilized in Eq. (1). All three net coefficients in this new series are set equal to zero. This gives rise to a set of three homogenous algebraic equations relating the Fourier driving coefficients E_{m11} (1), E_{m11} (2), ... etc. Coefficients of these homogeneous algebraic equations are entered into the appropriate matrix segment at the appropriate location.

It will be recalled that contributions of the first and second building blocks to bending moment along the edge, $\eta = 1$, are provided by Eq. (13), where the dimensionless bending moment is expressed as Mb^2/a_1D. Contributions of the third building block appear in the third segment of the first row. They are available from Eq. (22), however, they must be multiplied by the factor b/a_1, in order to obtain the dimensionless form Mb^2/a_1D. The same rules apply in generating the second row of segments of the matrix.

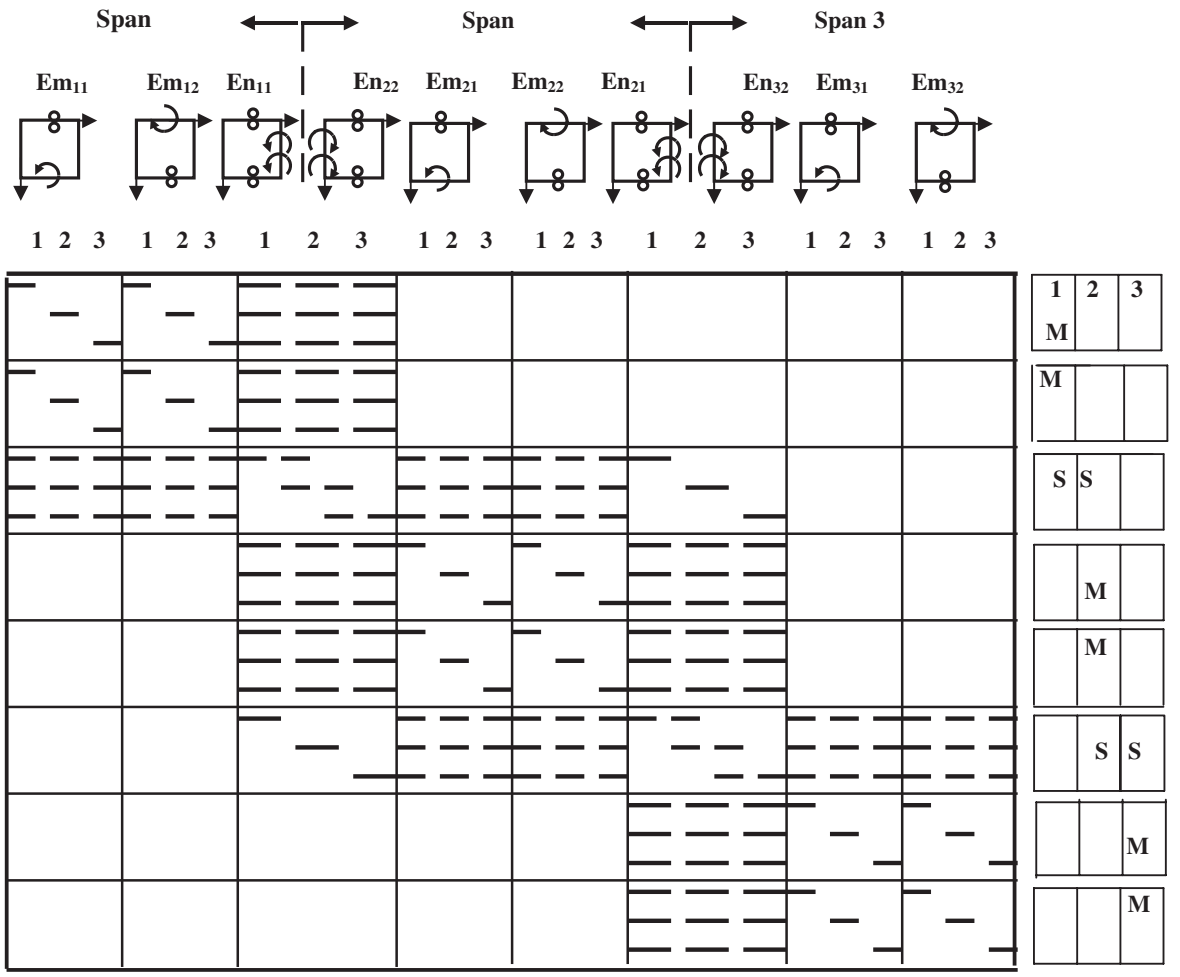

Fig. 4. Schematic representation of eigenvalue matrix used in analysing three-span deck behaviour.

The third row of matrix segments is based on continuity of slope across the interface between the first and second spans. All building blocks of the first and second spans will contribute toward slope at the interface.

Before discussing generation of elements of these segments we must recognize that due to continuity of bending moment across the interface, the coefficients E_{n11} and E_{n22} of the third and fourth building blocks will not be independent. For any term "n" in the series the moment along the interface experienced by the third building block is expressed as (Eq. (19))

$$\frac{Ma_1^2}{bD} = E_{n11}(n)\cos n\pi\eta. \tag{23}$$

The corresponding dimensionless moment distribution in the fourth building block is written as

$$\frac{Ma_2^2}{bD} = E_{n22}(n)\cos n\pi\eta. \tag{24}$$

Since the basic moments, M, are equal at the interface, it follows that

$$E_{n22}(n) = E_{n11}(n)(a_2^2/a_1^2). \tag{25}$$

The net contributions of the first three building blocks to interface slope, minus the net contribution of the next four must equal zero. Accordingly, we expand in a cosine series the difference in these net contributions and require each coefficient in this new series to vanish. This gives rise to the set of homogeneous algebraic equations on which the elements of the third row of segments are based.

Two points must be made clear here. First, we wish to equate actual basic slopes. Taking derivatives of the form, $\partial W/\partial\xi$, for the first two building blocks gives us this basic slope, since both W and the coordinate ξ are non-dimensionalized by the edge length, "a_1". The third and fourth building blocks have their lateral displacement non-dimensionalized by edge length "b". Accordingly, their contributions to slope obtained by differentiating as $\partial W/\partial\xi$, etc., must be multiplied by b/a_1, and b/a_2, respectively.

The first two matrix segments below the third building block pertain to it only. It will be noted that a pair of elements are indicated at each position along the diagonal of the third row segment immediately below the third and fourth building blocks. The element on the left pertains to the third building block contribution while the other element pertains to the fourth building block contributions. This is the only row of segments where coupling between the first and second span building blocks occurs.

Segments of rows four and five of the matrix pertain to the zero moment condition to be enforced along the free edges of the centre span. Segments in these rows, immediately below the third and fourth building blocks, pertain to the fourth building block contributions only. In summary, all elements in the third column of matrix segments pertaining to the third building block must be multiplied by the factor, b/a_1, while all elements pertaining to the fourth building block must be multiplied by $(a_1/a_2)^2 b/a_2$.

It is expected that with this pattern established the reader will be able to generate the appropriate eigenvalue matrix regardless of the number of spans involved. Only the building block aspect ratios, and hence the interface column multiplication factors, will change as we move down and across to the right as the matrix is generated.

Attention should be focussed on the row of subscripts immediately underneath the building block figures at the top of Fig. 4. These subscripts pertain to the driving coefficients E_{m11}, E_{m12}, E_{n11}; E_{m21}, E_{m22}, E_{n21}; E_{m31}, and Em_{32}. They do not pertain to the driving coefficients E_{n22}, and E_{n32} immediately to the right of the inter-span divisions. As pointed out above, once the driving coefficients related to the building blocks immediately to the left of the inter-span divisions are known, driving coefficients of the adjacent building blocks immediately to the right are uniquely established (see Eq. (25) for example).

When conducting the study of a mode shape associated with any eigenvalue, one of the non-zero driving coefficients is set equal to unity and the resulting set of non-homogeneous algebraic equations relating the other unknown coefficients is solved. Finally, values are assigned to the driving coefficients of building blocks immediately to the right of the inter-span division lines. It will be obvious that for a three-span analysis, using K terms in the building block solution expansions, the eigenvalue matrix will be of dimensions $8K \times 8K$.

At the time of writing a self-indexing computer scheme has been developed which will generate the matrix for any number of spans. Eigenvalues are obtained, of course, by searching for those values of the parameter, λ^2, which cause the determinant of the eigenvalue matrix to vanish.

3. Computed results based on multi-span approach

The reader will recognize that there are a certain limited number of eigenvalues and mode shapes for the family of problems under investigation which are available from simple Lévy type solutions. These are available through essentially exact solutions to the free vibration of rectangular plates with one pair of opposite edges simply supported and the other edges free. These simple solutions are available only when all spans of the multi-span plate have the same aspect ratio. In such cases the fundamental frequency and mode shape is available.

Consider, for example, the first mode vibration of a three-span plate, with spans of aspect ratio equal to 1.0. Consider also, the free vibration of a plate with two opposite simply supported edges, two free edges, and the ratio of length along the free edges to length along the simply supported edges = 3.0. In one of the higher modes of vibration of this latter plate, there will be two equi-spaced node lines running parallel to the simply supported edges and no node lines running parallel to the free edges. It will be obvious that this problem corresponds exactly to the three span problem discussed immediately above and eigenvalues, will be the same for both problems. We would say that the inter-span supports are in-active in such cases. Both problems will also have corresponding modes when in addition to the two node lines running parallel to the simply supported edges as discussed above, there is a single node line running parallel to the free edges.

These exact solutions, which the reader will have no trouble identifying when they apply, serve a valuable role as they provide reference points against which results computed by the present method may be compared. A large array of these pre-computed eigenvalues are listed in Ref. [1]. They will be referred to here as "exact eigenvalues".

All computations based on the present method have been performed with the use of seven terms in the building block solutions ($K = 7$). It has been found that use of more terms will not change the first four digits in computed eigenvalues.

The reader will understand that with the many parameters appearing in the multi-span plate, there is no possibility of storing a comprehensive listing of eigenvalues, even for the three-span plate. For this reason, only a limited amount of data will be presented here for the purposes of helping to verify the validity of the analysis. This same data will provide reference values against which the findings of other researchers may be compared.

In Table 1 computed eigenvalues are tabulated for the first six free vibration modes of a three-span plate. Here the aspect ratios of the first and third span are fixed at 1.0, while the aspect ratio of the central span is allowed to vary from 1.0 to 1.1. In the interest of consistency all tabulated eigenvalues are non-dimensionalized with respect to the fixed bridge deck width "b". A value of 0.333 has been used for the Poisson ratio for all computations.

Table 2 differs from Table 1 only in that in this latter table the inverse of the central span aspect ratio is allowed to vary from limits of 1.0 to 1.1. Since we have chosen a value of K equals 7 for preparation of the data of these tables the associated eigenvalue matrices will be of dimensions 56×56.

Table 1
First six eigenvalues, $\lambda_b^2 = \omega b^2\sqrt{\rho/D}$, computed for three-span continuous plate ($\phi_1 = \phi_3 = 1.0,\ 1.0 \leqslant \phi_2 \leqslant 1.1$)

Mode	ϕ_2					
	1.0	1.02	1.04	1.06	1.08	1.10
1	9.568	9.693	9.809	9.917	10.02	10.11
2	12.36	12.39	12.43	12.46	12.49	12.52
3	15.88	16.02	16.14	16.25	16.35	16.44
4	18.04	18.07	18.09	18.11	18.13	18.15
5	18.18	18.62	19.07	19.53	20.01	20.49
6	22.96	23.44	23.93	24.45	24.98	25.52

Table 2
First six eigenvalues, $\lambda_b^2 = \omega b^2\sqrt{\rho/D}$, computed for three-span continuous plate ($\phi_1 = \phi_3 = 1.0,\ 1.0 \leqslant 1/\phi_2 \leqslant 1.1$)

Mode	$1/\phi_2$					
	1.0	1.02	1.04	1.06	1.08	1.10
1	9.568	9.437	9.302	9.164	9.022	8.877
2	12.36	12.32	12.29	12.25	12.21	12.18
3	15.88	15.73	15.57	15.40	15.22	15.03
4	18.04	17.77	17.39	17.03	16.71	16.40
5	18.18	18.02	18.00	17.98	17.96	17.94
6	22.96	22.51	22.11	21.74	21.40	21.10

Exact eigenvalues for the continuous plate of three equal spans are available from Ref. [1] as 9.568 and 15.88. The first corresponds to the three-span plate fundamental mode, while the second corresponds to the lowest three-span mode with central node line running parallel to the free edges. It is seen that those are the first and third eigenvalues of the three equi-span plates.

Further verification tests of the data of Tables 1 and 2 are possible. With the first and third span geometries fixed, and the aspect ratio ϕ_2 allowed to increase, we recognize that the length of the central span becomes shorter ($\phi_2 = b/a_2$), the three-span plate assembly thus becomes stiffer and we expect the plate natural frequencies to rise. In fact, this is seen to be the case in Table 1.

Conversely, as the aspect ratio, ϕ_2, decreases, the eigenvalues should decrease, as they do in Table 2.

It is observed, however, that the fourth mode eigenvalue of Table 1 is extremely insensitive to change in the centre span length in the range of aspect ratios studied.

It is appropriate at this time to elaborate upon the significant advantages of the present multi-span analysis over the analysis centred around a single deck plate with intermediate transverse line supports as described in Ref. [3].

In this earlier approach, instead of analysing each deck span separately and enforcing inter-span continuity conditions, the entire deck is treated as a single long thin plate with line support applied at each inter-span location. At each line support a condition of zero plate lateral

displacement is enforced. Both the earlier analytical approach and the present entirely different approach were applied to identical multi-span plate free vibration problems. Agreement between the two sets of results obtained was excellent. In fact, for first mode vibration computed eigenvalues agreed to four significant digits. This agreement, achieved utilizing two entirely different approaches, attests to the accuracy of both the earlier and the present analytical methods.

Let us suppose now that we wish to analyse a deck of many spans, utilizing the earlier approach where we consider a simple long plate with numerous transverse line supports [3]. Let us suppose for illustrative purposes that the span lengths are equal to the width of the deck and it is composed of 15 spans. The aspect ratio of the full deck plate, ϕ, would then equal one fifteenth. Referring now to Eqs. (20) and (21) it is seen that the argument, β_n, associated with these equations, and which is inversely proportional to the full plate aspect ratio, will become massive. Furthermore, the quantity $m\pi$, and hence $n\pi$, must now take on an extremely high value. This is because 'm' must be large enough so that a sufficient number of trigonometric function half-waves will be contained in each individual span. This second requirement will lead to an even more massive value for the quantity β_n.

Referring again to Eqs. (20) and (21) we note that the arguments utilized in the hyperbolic functions will thus take on massive values leading to computer overflow and inevitable computational roundoff errors. All of these difficulties are avoided for bridge decks of high numbers of spans through exploitation of the multi-span analytical approach as described here.

Results of mode shape studies for the first three modes of the three-span plate with, $\phi_1 = \phi_3 = 1.0, \phi_2 = 1.1$, are presented in Figs. 5–7. Similar results for the next three higher modes with a value of $\phi_2 = 1.0$ instead of 1.1, are presented in Figs. 8–10.

As expected, due to choice of aspect ratios, all modes possess symmetry, or antisymmetry, with respect to the deck central axes. Antielastic bending due to Poisson effects is observable in a number of the mode shapes.

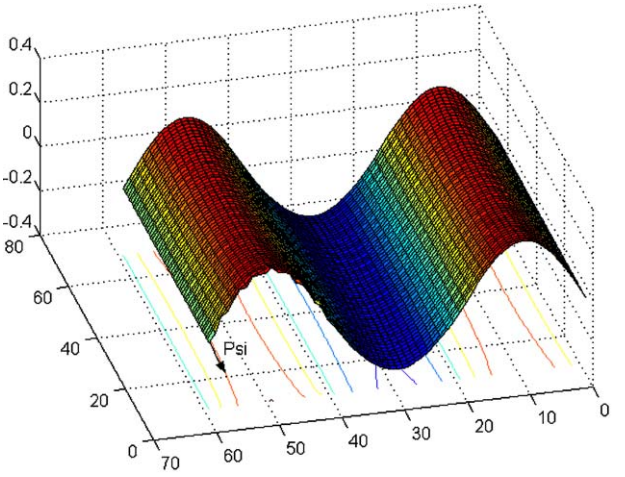

Fig. 5. Computed mode shape for first mode vibration, $\phi_1 = \phi_3 = 1.0$, $\phi_2 = 1.1$.

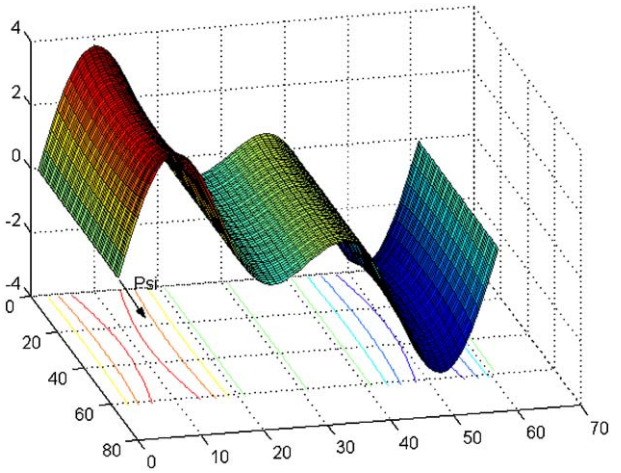

Fig. 6. Computed mode shape for second mode vibration, $\phi_1 = \phi_3 = 1.0$, $\phi_2 = 1.1$.

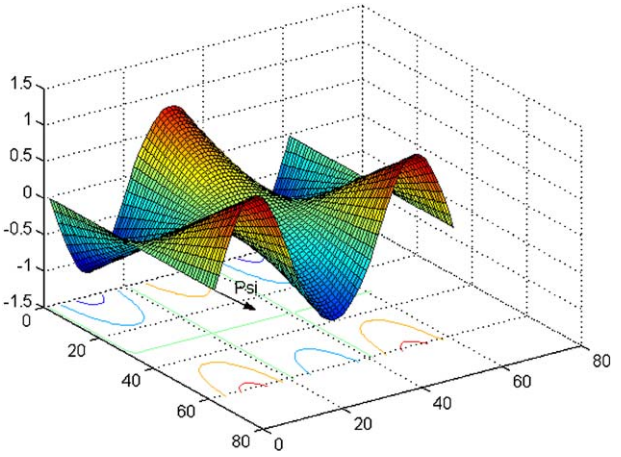

Fig. 7. Computed mode shape for third mode vibration, $\phi_1 = \phi_3 = 1.0$, $\phi_2 = 1.1$.

4. Discussion and conclusions

The superposition method as exploited here is shown to provide an orderly analytical method for computation of accurate natural frequencies and mode shapes of multi-span bridge decks. The present study differs significantly from an earlier one employing the superposition method in that here a span-by-span analysis is conducted. The vast computational advantages of the present approach over the earlier study, when large numbers of spans are involved and high accuracy is required, are discussed. Nevertheless, excellent agreement is obtained when results computed for bridge decks of up to three spans are compared.

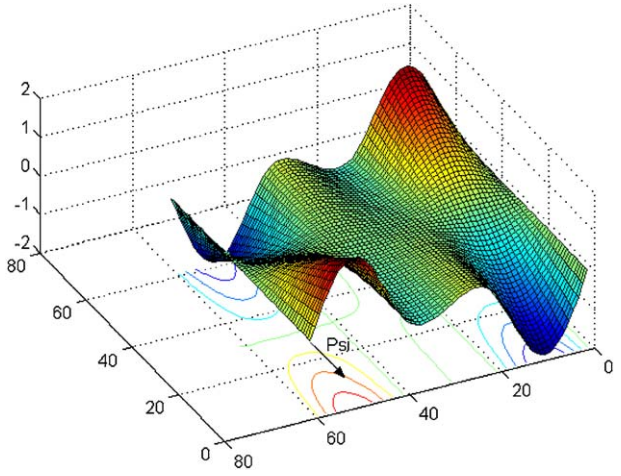

Fig. 8. Computed mode shape for fourth mode vibration, $\phi_1 = \phi_2 = \phi_3 = 1.0$.

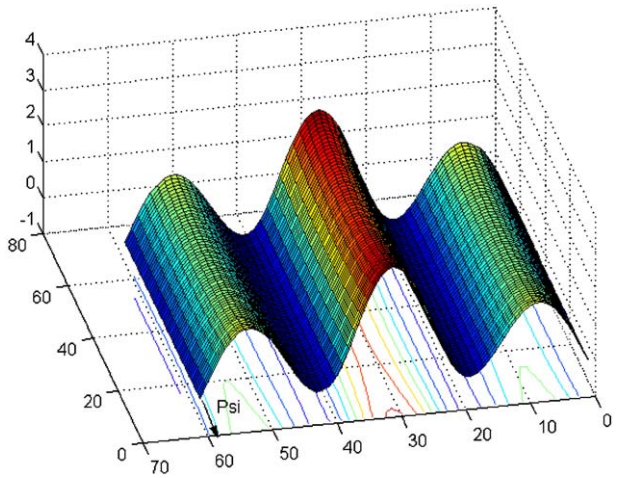

Fig. 9. Computed mode shape for fifth mode vibration, $\phi_1 = \phi_2 = \phi_3 = 1.0$.

It is recognized that a certain amount of idealization has been introduced in this study of the problem where the deck is treated as a series of thin isotropic plates. Nevertheless, this simplified model has deliberately been utilized here so that the analytical procedure may be verified and wherever possible, computed eigenvalues may be compared with known exact values.

As indicated earlier, the analysis may be easily extended to handle orthotropic plates [4]. It has already been extended to analyse similar multi-span decks with vertical elastic cable support and rigid cross members at inter-span locations [5]. For the present it is intended to utilize the simplified model to permit investigation of actual bridge dynamic behaviour by means of modal analysis. Further complications of the type discussed immediately above will be introduced as required.

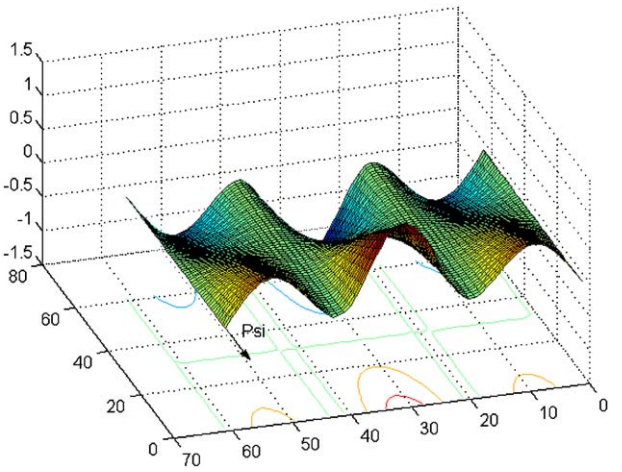

Fig. 10. Computed mode shape for sixth mode vibration, $\phi_1 = \phi_2 = \phi_3 = 1.0$.

It is important to recall that free vibration solutions provided by the method discussed here satisfy exactly the governing differential equation throughout the entire domain of each span. Convergence is rapid, thereby permitting the satisfaction of all prescribed boundary conditions to any desired degree of accuracy.

References

[1] D.J. Gorman, *Free Vibration Analysis of Rectangular Plates*, Elsevier North-Holland Inc., New York, 1982.
[2] D.J. Gorman, *Vibration Analysis of Plates by the Superposition Method*, World Scientific Publishing Co. Pte. Ltd., Singapore, 1999.
[3] D.J. Gorman, A highly accurate and efficient analytical approach to bridge deck free vibration analysis, *Journal of Shock and Vibration* 7 (2001) 399–412.
[4] D.J. Gorman, Free vibration of orthotropic cantilever plates with point supports, *Journal of Engineering Mechanics, American Society of Civil Engineers* 2 (8) (1995) 851–857.
[5] D.J. Gorman, Analytical study of free vibration of cable supported bridges, *Japanese Society of Mechanical Engineers, International Series C* 45 (1) (2002) 40–53.